

UDC 66.01

DOI: 10.15587/1729-4061.2022.269844

SYNTHESIS OF NANOCOMPOSITES REDUCED GRAPHENE OXIDE-SILVER NANOPARTICLES PREPARED BY HYDROTHERMAL TECHNIQUE USING SODIUM BOROHYDRIDE AS A REDUCTOR FOR PHOTOCATALYTIC DEGRADATION OF Pb IONS IN AQUEOUS SOLUTION

Nurhayati Indah Ciptasari
Master of Science***

Research Center for Metallurgy*

Murni Handayani

Corresponding author

Doctor of Philosophy (PhD)

Research Center for Advanced Materials*

Caesart Leonardo Kaharudin

Bachelor of Science**

Afif Akmal Afkauni

Bachelor of Science**

Adhi Dwi Hatmanto

Doctor of Philosophy, PhD**

Isa Anshori

Doctor of Philosophy, PhD

Department of Biomedical Engineering

School of Electrical Engineering and Informatics

Research Center for Nanosciences and Nanotechnology (RCNN)

Bandung Institute of Technology

Jl. Ganesa No.10, Lb. Siliwangi, Kecamatan Coblong, Kota Bandung, Jawa Barat, Indonesia, 40132

Ahmad Maksun

Doctor of Engineering, Assistant Professor

Research Center for Eco-Friendly Technology

Department of Mechanical Engineering

Politeknik Negeri Jakarta

Jl. G.A. Siwabessy Kampus Baru UI Depok, Jawa Barat, Indonesia, 16425

Rini Riastuti

Doctor of Engineering, Associate Professor

Johny Wahyuadi's Laboratory***

Johny Wahyuadi Soedarsono

Doctor of Engineering, Professor

Johny Wahyuadi's Laboratory***

*National Research and Innovation Agency (BRIN)

Kawasan Puspipstek, 470, Building, Tangerang Selatan, Banten, Indonesia, 15314

**Department of Chemistry

Universitas Gadjah Mada

Bulaksumur, Daerah Istimewa Yogyakarta, Indonesia, 55281

***Department of Metallurgy and Materials

Universitas Indonesia

Kampus Baru UI Depok, Jawa Barat, Indonesia, 16424

Heavy metals are pollutants that are harmful to living things and the environment can be degraded by microbes or understood by other living things so that they can cause health problems. One of the heavy metals that is often found in wastewater is lead. Lead is widely used in the manufacture of batteries, metal products such as ammunition, cable coatings, Polyvinyl Chloride (PVC) tubing, solder, chemicals and dyes

This use causes humans to be exposed to large amounts of lead. One method to deal with lead pollution is to use photocatalysts. Photocatalysts react with heavy metals and reduce them so that the level of toxicity becomes lower than before through photocatalytic reactions. In this study, synthesis of reduced graphene oxide/silver nanoparticle nanoparticles was performed by facile hydrothermal methods for photocatalytic degradation of Pb ion. The characterization results indicate that the synthesis has been successfully carried out. The successful result of rGO/AgNPs nanocomposites synthesis was proved by several techniques such as X-ray diffraction analysis, Raman, UV-Vis spectroscopy, Scanning Electron Microscopy (SEM) and Energy Dispersive X-Ray analysis (EDX). This indicates the presence of these groups in the graphene oxide and rGO/AgNPs samples, respectively. The resulting rGO/AgNPs nanocomposite has an absorbance peak at a wavelength of 267 nm. The diffraction peaks for nanocomposites rGO/AgNPs and their Miller indices were 38.08° (111), 44.16° (200), 64.44° (220), and 77.44° (311). The Raman spectra of rGO/AgNPs exhibits D bands at 1334,13 with intensity of $630,60\text{ cm}^{-1}$ and G band at 1594,61 with intensity of $477,29\text{ cm}^{-1}$. The ID/IG ratio rGO/AgNPs-NaBH₄ is ~1,32. Furthermore, the photocatalytic activity test results showed that the rGO/AgNPs nanocomposite was able to reduce Pb²⁺ to Pb with a maximum exposure time of 1.5 hours

Keywords: lead, reduced graphene oxide, silver nanoparticles, rGO/AgNPs nanocomposite, sodium borohydrate

Received date 07.10.2022

How to Cite: Ciptasari, N. I., Handayani, M., Kaharudin, C. L., Afkauni, A. A., Hatmanto, A. D., Anshori, I., Maksun, A., Riastuti, R., Soedarsono, J. W. (2022). Synthesis

Accepted date 09.12.2022

of nanocomposites reduced graphene oxide-silver nanoparticles prepared by hydrothermal technique using sodium borohydrate as a reductor for photocatalytic degrada-

Published date 30.12.2022

tion of pb ions in aqueous solution. Eastern-European Journal of Enterprise Technologies, 6 (5 (120)), 54–62. doi: <https://doi.org/10.15587/1729-4061.2022.269844>

1. Introduction

Heavy metals are harmful to living things and the environment because they cannot be degraded by microbes

or digested by other living things. As a result, it causes the accumulation of heavy metals in living body tissues (bio-accumulation) which can cause health problems [1]. Heavy metals that are often found in wastewater are arsenic, cadmi-

um, chromium, copper, lead, nickel, and zinc. All these heavy metals can cause harmful health effects. Lead (Pb) is one of the most dangerous heavy metals. Lead is used in the manufacture of batteries, metal products such as ammunition, cable coatings, Polyvinyl Chloride (PVC) pipes, solder, chemicals and dyes. This use causes humans to be exposed to large amounts of lead. Lead plays no biological role at all. However, when absorbed by cells, lead competes with other metal ions such as calcium, iron, and magnesium for binding to cell receptors. Thus, it interferes with cellular metabolic processes and damages cells [2].

One method to deal with lead pollution is by the use of a photocatalyst.

Photocatalyst is a catalytic material that is active when exposed to light. The electrons in the valence band of the photocatalyst will be excited to the semiconductor band to produce one electron hole and one unpaired electron. Electrons and electron holes can undergo recombination, which reverses the excitation [3]. The existence of these holes and electrons makes photocatalysts able to reduce or oxidize other chemical species. The reaction occurs depending on the reduction potential of the chemical species. Factors that affect photocatalyst activity are temperature, concentration of reactants and photocatalysts, pH, light intensity, and the presence of additives such as oxidants that can prevent recombinants [4].

Photocatalytic technology is an environmentally friendly technology to convert pollutants in wastewater into products that are not harmful to the environment [5–7]. TiO_2 , recently emerged as an excellent semiconductor material for photocatalysts, exhibits efficient, chemically stable, non-toxic and non-polluting performance [8–11]. However, due to the relatively high rate of electron-hole pair recombination and apparently low light utilization, its real-life applications are very limited [12, 13].

Graphene is an emerging material later in the current decade. In recent years, graphene has been widely used for photocatalytic applications due to its large surface area, high electron mobility, strong adsorption capacity, and easy chemical modification [14–16]. Graphene and its derivatives (e. g., graphene oxide, GO; and reduced graphene oxide, rGO) are carbon monolayer materials, 2D sp^2 which have attractive, unique and extraordinary properties, so they have great potential to be used for various applications such as in batteries, polymer chargers, sensors, energy conversion, and energy storage devices [17, 18]. Graphene has a Young's Modulus and Strength of ~ 130 GPa has electron mobility at room temperature of $\sim 2.5 \times 10^5 \text{ cm}^2 \text{V}^{-1} \text{ s}^{-1}$ and a large specific surface area (theoretically $2630 \text{ m}^2/\text{g}$ for single-layer graphene which are commonly applied to sensors [19–21]. Graphene derivatives have several beneficial effects on photocatalytic performance by creating a synergy between the semiconductor and the carbon phase [18]. This is mainly due to a decrease in the energy band gap of the composite catalyst, an increase in the adsorption properties of the material, and charge of transport separation. Incorporation of graphene derivatives with their composites for semiconductor photocatalysts can improve photocatalytic performance because of this combination increase photodegradation, adsorption capacity, photostability and light absorption [18].

Furthermore, rGO has an important advantage, namely the possibility of obtaining a hydrophilic surface from reduced oxygenated graphene, at a relatively low production cost [22]. These surface groups can be used to facilitate

anchoring of semiconductors and metal nanoparticles and even for the assembly of macroscopic structures, which are relevant for developing highly efficient photocatalysts [23]. The study showed that reduced graphene oxide/titanium dioxide (rGO/ TiO_2) composites were effective as photocatalysts for the photocatalytic degradation of methyl orange [5]. Excited electrons from TiO_2 flow to rGO, thereby inhibiting recombination and increasing photocatalyst activity. Previous studies have proven that TiO_2 can remove Pb^{2+} from water [6].

Therefore, studies that are devoted to synthesize reduced graphene oxide/silver nanoparticles nanocomposites (rGO/AgNPs) as an alternative photocatalytic material for waste treatment especially for degradation of Pb ions. Graphene is a two-dimensional enclosed hexagonal honeycomb lattice with sp^2 hybridization. Graphene has high surface area, excellent electrical, optical and mechanical properties [24]. Graphene has been considered as an attractive matrix of nanocomposites for the integration with the metal nanoparticles (NPs) in realizing further novel and superior properties for various specific applications. Silver nanoparticles (AgNPs) are one of the most extensively applied nanomaterials owing to their, high catalytic activity, large specific surface area and antibacterial capability [25]. By combining the two materials of reduced graphene oxide with silver nanoparticles, it would give rise to synergistic effect for enhancing photocatalytic behavior.

2. Literature review and problem statements

The paper [8] reported the photocatalytic of TiO_2 /Carbon-Dots using a facile hydrothermal-calcination synthesis technique for the degradation of Gemfibrozil under simulated sunlight irradiation. Carbon-Dots have been chosen in this paper to combine with TiO_2 because carbon dots demonstrated to possess excellent upconversion photoluminescence. That is, lower-energy light or in visible or near-infrared light from 500 to 1000 nm can be converted to higher-energy light (ultraviolet or visible light from 325 to 425 nm) via the multiple photon absorption property of Carbon-Dots. The upconversion function of Carbon-Dots enables the visible and near-infrared spectrum of sunlight to be utilized, obtaining in an increase of photocatalytic efficiency. The result showed that under simulated sunlight irradiation, a very low Carbon-Dots loading of 5.0 wt % obtained in a 2.3 times faster reaction rate for photodegradation of gemfibrozil than pristine TiO_2 . The faster reaction is driven from oxidative species, particularly OH as the most important reactive species mediating the photocatalytic degradation of gemfibrozil. However, this method needs further investigation using electron spin resonance (ESR) which could determine the most important reactive species of photocatalytic degradation. In addition, quantum chemical calculation is required to verify the degradation mechanism.

The paper [9], reported a series of GO/ TiO_2 / Bi_2WO_6 nanocomposite photocatalyst, which was synthesized successfully using one-step hydrothermal technique for the application in degradation of ethylene. The influence of the graphene oxide addition to the nanocomposite for degradation of the ethylene was investigated. The result revealed that the degradation of ethylene under visible light is high. The addition of 0.75 % of GO is the highest for ethylene

degradation at 5.7 times, 2.8 times and 1.3 times that of pure TiO_2 , Bi_2WO_6 and $\text{TiO}_2/\text{Bi}_2\text{WO}_6$ respectively. The reason of the highest result due to the combination of GO with $\text{TiO}_2/\text{Bi}_2\text{WO}_6$ obtaining multiple heterojunctions, so that the bandwidth smaller is omitted. Besides that, the addition of GO diminishes the average grain size of the nanocomposite size, and creates an interfacial interaction with $\text{TiO}_2/\text{Bi}_2\text{WO}_6$, inhibiting the recombination of photogenerated electron-hole pairs and enhance the photocatalytic activity. Nevertheless, this technique necessitated high costs, impractical and difficult to control the system during the reaction process because the photocatalytic degradation of the ethylene test required specific platform, which consisted of a photocatalytic reaction system and a constant-temperature water-circulation system. The photocatalytic reaction system is composed of an ultrahigh-pressure Xe lamp (light intensity 500 W), UV cutoff filter, reaction film support, photocatalytic film gas-circulation device, and photocatalytic reactor. Besides that, in order to evaluate the photocatalytic activity of $\text{TiO}_2/\text{Bi}_2\text{WO}_6$, the materials has to be loaded on an activated carbon fiber as photocatalytic film prepared by dip coating which needs to control the rate of coating in order to get the best loading of the materials with homogeneous and desired thickness.

The paper [11] developed a visible-light-driven magnetically recoverable nitrogen doped TiO_2 -based nanophotocatalyst ($\text{N-TiO}_2@\text{SiO}_2@\text{Fe}_3\text{O}_4$) for degradation of pharmaceuticals (ibuprofen and carbamazepine) and a personal care product (benzophenone-3) by fine-tuning the pertinent factors such as calcination temperature, Fe_3O_4 loading, and nitrogen doping. Nanophotocatalyst performance on ibuprofen was studied using two visible light sources, i.e., compact fluorescent lamps (CFLs) and light emitting diodes (LEDs) of similar irradiance. The result showed that CFLs of irradiance $320 \mu\text{W cm}^{-2}$ and peak emissive wavelength 543 nm served as a better source producing the highest degradation of 94 %. Besides that, nanophotocatalyst performance on benzophenone-3 within 5 h under visible light emitted by CFLs give the degradation of 93 %. The degradation of 71 % for carbamazepine within 9 h was observed under visible light emitted by CFLs. This result revealed that the superparamagnetic behavior of the nanophotocatalyst enabled its successful magnetic separation (95 % efficiency) from the suspension within 20–25 min under an electromagnetic field of ~ 200 mT. In this method, different temperature of the calcination process was required (400 and 500 °C) in order to enhance the photocatalytic efficiency of the nanophotocatalyst. This means that the preparation of the nanophotocatalyst materials needs high temperature to obtain higher efficiency.

The paper [16] reported the rGO- TiO_2 hybrid nanocomposites prepared by facile hydrothermal technique and combined with pulsed discharge plasma (PDP) for synergistic degradation of fluoroquinolone (FQ) antibiotic. Flumequine (FLU), a representative of FQ, is selected as the target compounds. The result showed that the highest removal efficiency can reach 99.4 % in PDP/graphene- TiO_2 system with 5 % graphene content, which is 23.7 % and 34.6 % higher than that in PDP/ TiO_2 system and sole PDP system, respectively. Correspondingly, the kinetic constant is 3.5 and 4.6 times higher than that in PDP/ TiO_2 system and sole PDP system, respectively. This will provide new insights in the application of graphene-based nanocomposites in PDP systems as a promising methodology for the reme-

diation of organic contaminants in water. Even though the hybrid nanocomposites show promising result, this approach need pulsed discharge plasma to make synergetic effect in order to enhance the photocatalytic performance.

The paper [26] reported the advantages of CuO, combining with GO, and synthesized $\text{TiO}_2/\text{rGO}/\text{CuO}$ nanocomposites by a hydrothermal method for the reduction of Cr(VI). A series of products with additive amount of $\text{CuSO}_4 \cdot 5\text{H}_2\text{O}$ and GO were prepared. The composite is denoted as TgxCy , where x and y represent the amount of GO aqueous solution in volume and $\text{CuSO}_4 \cdot 5\text{H}_2\text{O}$ in weight, respectively and compared their photocatalytic property. The result showed that under visible light irradiation, TG_2C_8 can completely reduce in 100 % of the Cr(VI) (100 ppm) solution in 80 min, and the photoreduction conversion rates of Cr(VI) on TG_2C_8 are 4.9 and 29.4 times those of P25 and pure TiO_2 , respectively. TG_2C_8 composites is attributed to the acceleration of e^- and h^+ pair separation by CuO and the acceleration of effective $e^+ - h^-$ transfer by rGO. Therefore, $\text{TiO}_2/\text{rGO}/\text{CuO}$ nanocomposites showed excellent property under visible light. From the result, it shows that pure TiO_2 give low efficiency compared with the $\text{TiO}_2/\text{rGO}/\text{CuO}$ nanocomposites. The efficiency of the photocatalytic reduction of Cr(VI) by neat TiO_2 is 63.23 %. Therefore, further study to explore nanocomposite materials with enhance photocatalytic activity is required.

Based on literature review mentioned above, photocatalysts materials were TiO_2 based-materials for the application of photocatalytic performances in degradation of pharmaceuticals, personal care product and heavy metal for waste treatment. The application of photocatalyst materials to treat heavy metal waste pollution in water was promising. Photocatalyst will reduce heavy metal ions in water so that heavy metals are no longer dissolved. Photocatalysts can also mineralize existing heavy metals (remediation) making it easier to remove them from water [27]. However, TiO_2 photocatalyst is exclusively activated with UV light ($\lambda \leq 380$ nm). The photocatalytic activity of TiO_2 under natural solar irradiation is largely limited [26]. Thus, it is highly desirable to design and seek efficient photocatalysts materials for the waste treatment under sunlight irradiation. Further research is needed regarding the handling of heavy metal atoms by photocatalyst materials other than TiO_2 .

Silver nanoparticles (AgNPs) are antimicrobial substances, which have the ability to inhibit or kill microbial growth with relatively little toxicity to humans. Therefore, silver nanoparticles are used in the disinfection process in water and wastewater treatment. Nanoparticles (AgNPs) exhibit attractive quantum characteristics, allowing for large specific surface area, small particle diameter, fast electron transfer capability, etc. AgNPs are also known to have high stability, good electrical conductivity, good light absorption, and high sensitivity [28]. Therefore, the addition of AgNPs can increase the photocatalytic activity of a material. The combination of AgNPs with reduced graphene oxide (rGO) by exploiting the large specific surface area and the effective built-in electric field of rGO forming binary nanocomposite can enhance the photocatalytic performance. The prepared binary nanocomposites of rGO/AgNPs was conducted with in-situ reaction which is facile and reduced the synthesis time duration. In addition, the photocatalytic activity test of the nanocomposites of rGO/AgNPs for degradation of Pb ions in this method was performed in room temperature, which is easy, low cost and very practical.

3. The aim and objectives of the study

The aim of this study is to synthesize rGO/AgNPs nanocomposites with NaBH_4 reductor using the hydrothermal method and to test their photocatalytic activity against Pb ions. So that it can be investigated the performance of the effectiveness of photocatalytic rGO/AgNPs to make it possible alternative photocatalytic materials for waste treatment.

To achieve the aim, the following objectives are set:

- to investigate the properties of the synthesis of Graphene Oxide and rGO/AgNPs using X-Ray Diffraction Analysis (XRD), Scanning Electron Microscope (SEM), Raman Spectroscopy and UV-Vis spectrophotometer;

- to investigate the influence of UV light exposure time on the photocatalytic test process.

4. Materials and methods of research

4. 1. Object and hypothesis of the study

In this study, materials rGO/AgNPs nanocomposites are used as photocatalysts for degradation of Pb ions in aqueous solution. The rGO/AgNPs nanocomposite was prepared from reduced graphene oxide and silver nanoparticles. Reduced graphene oxide (rGO) has the combined properties of graphene and graphene oxide. Reduction causes rGO to have better electrical conduction ability and crystalline structure than graphene oxide but still has functional groups such as graphene oxide [29]. Meanwhile, silver nanoparticles (AgNPs) are colloidal silver particles measuring 1 to 100 nm, with many benefits, especially in the health sector as anticancer and antimicrobial candidates. The rGO/AgNPs nanocomposite is also known to have high stability, electrical conductivity, absorb light well and have a high level of sensitivity. So the addition of AgNP can increase the photocatalytic activity of a material. It is thought that the increase in activity is due to the formation of high-energy electrons on the surface of AgNPs when AgNPs are exposed to light (localized surface plasmon resonance) [28]. Therefore, the study is devoted to the facile synthesis of rGO/AgNPs nanocomposites prepared by hydrothermal method, and the implementation of the alternative nanophotocatalytic technology in waste treatment that is more effective of rGO/AgNPs nanocomposites. That is, it is necessary to extend the understanding of physical, chemical and material properties of rGO/AgNPs nanocomposites and the effectiveness of the photocatalytic performance of the nanocomposites.

4. 2. Synthesis of graphite oxide

Graphite oxide was synthesized using the modified hummer method from the previous report [30, 31]. Amount of 1.5 g of graphite; 1.5 g NaNO_3 ; and 70 mL of H_2SO_4 mixed into a 1 L beaker (ice bath). After the temperature is below 20°C , 7.5 g of KMnO_4 is added slowly and then stirred for 2 hours. The temperature was increased to 37°C and stirred for 20 hours. The heater was turned off, and then 125 mL of distilled water was added to the solution and stirred for 30 minutes. Next, 10 mL of 30 % H_2O_2 and 400 mL of distilled water were added and stirred for 30 minutes. The solution was then allowed to

stand for one day. After settling, 5 drops of 2M HCl were added and stirred for 10 minutes. Then, the solution was allowed to stand for 3 hours, and the solids were separated and washed by centrifugation (7000 rpm, 15 minutes) until the solution was clear. The solid was dried in a furnace at a temperature of 75°C for 14 hours and characterized using UV-Vis spectrometer, XRD, and SEM.

4. 3. Synthesis of rGO/AgNP nanocomposites

The solution to be used is made first. 0.1M AgNO_3 solution was prepared by dissolving 1.7 g AgNO_3 in 100 mL of distilled water. 0.1 M NaBH_4 solution was prepared by dissolving 0.38 g NaBH_4 in 100 mL of distilled water. 0.5 g of graphene oxide was dissolved in 50 mL of distilled water and 50 mL of 96 % ethanol and sonicated for 20 minutes. Then 15 mL of 0.1 M AgNO_3 was added and stirred with a magnetic stirrer for 30 minutes. The solution was added with 25 % NH_3 until the pH was close to 10. Then, 30 mL of 0.1 M NaBH_4 solution was added. The solution was refluxed for 18 hours at 150°C . After completion, the precipitate was separated and washed by centrifugation until the pH of the supernatant was neutral. The solids resulting from the centrifugation were then dried in an oven at 75°C for 24 hours [25].

4. 4. Photocatalytic activity test

Amount of 0.01 g of rGO-AgNPs nanocomposite was weighed and dispersed in 5 mL of distilled water and then sonicated for 20 minutes. The dispersion was added to 50 mL of 10 ppm $\text{Pb}(\text{NO}_3)_2$ solution and stirred in the dark for 1 hour. The solution was then irradiated by UV for 3 hours. Every 30 minutes, 5 ml of the solution sample is taken to be tested for absorbance.

5. Research results of synthesis of nanocomposites reduced graphene oxide-silver nanoparticles

5. 1. Characterization result by X-Ray Diffraction, Scanning Electron Microscope, Raman and UV-Vis spectrophotometer

X-ray diffraction analysis (XRD) was used to observation of the starting material and the product were performed and to determine the crystal structure. The Fig. 1 shows the X-ray diffraction pattern of the nanocomposite of GO and rGO/AgNPs. X-ray diffraction analysis (XRD) was used to observation of the starting material and the product were performed and to determine the crystal structure.

In order to observe the morphology of grain rGO/AGNPs- NaBH_4 nanocomposite, analysis process was carried out by SEM. The analysis result of product obtained from synthesis, depicted in Fig. 2, 3.

The EDX analysis was performed on the grain surface to observe the elements on rGO/AGNPs. The EDX analysis results can be seen in Fig. 3.

In order to confirm the vibration spectra of rGO/AgNPs-rGO/AgNPs the synthesized composite compound, a Raman spectrum test was carried out (Fig. 4).

Characterization using UV-Vis spectrophotometer which is used to determine the band gap energy of the synthesis of GO and rGO/AgNPs compounds shown in Fig. 5.

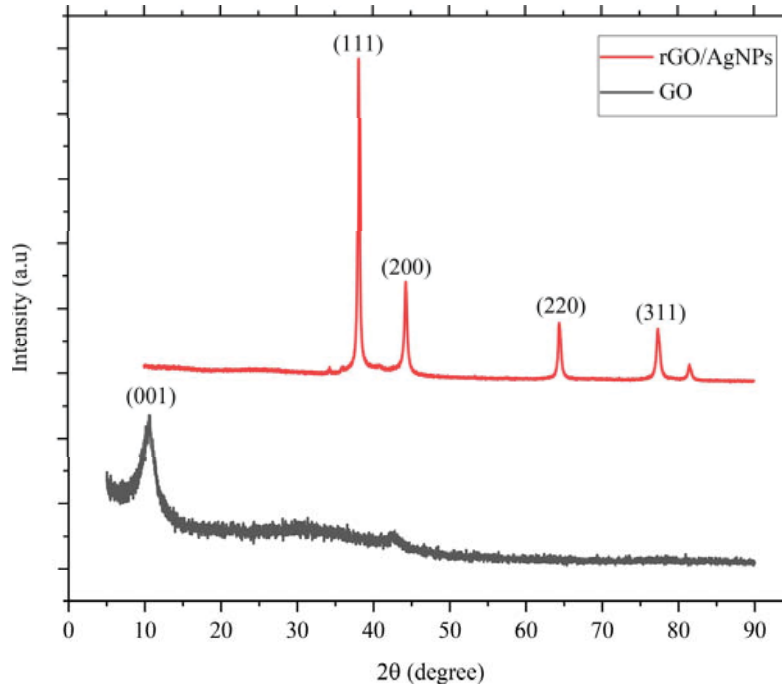


Fig. 1. X-Ray Diffraction characterization of graphene oxide and rGO/AgNPs-NaBH₄

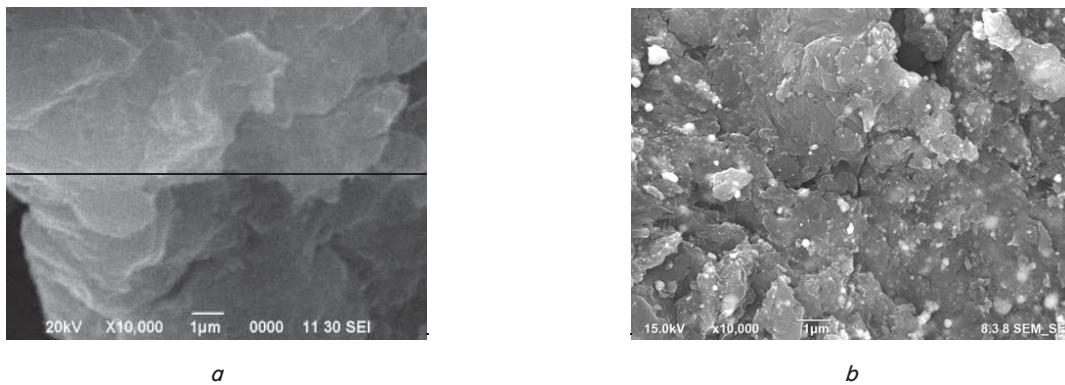


Fig. 2. Morphology observation with scanning electron microscope (SEM):
a – Graphene oxide with magnification 10.000X;
b – rGO/AgNPs nanocomposite with magnification 10.000X

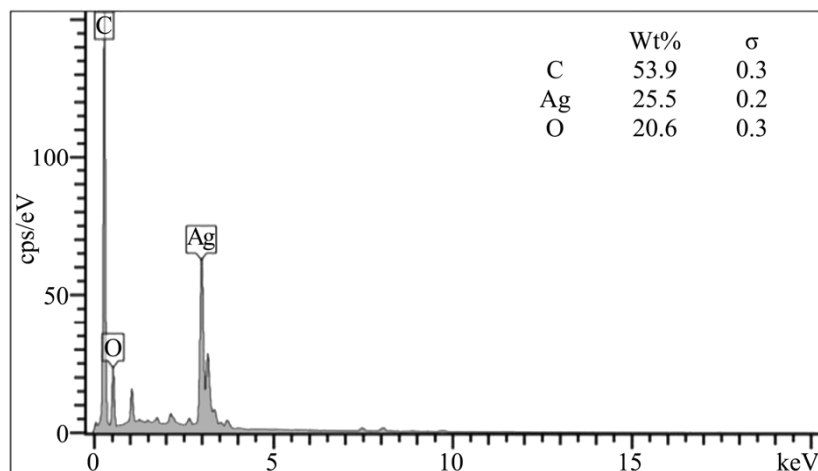


Fig. 3. Energy dispersive X-Ray analysis result

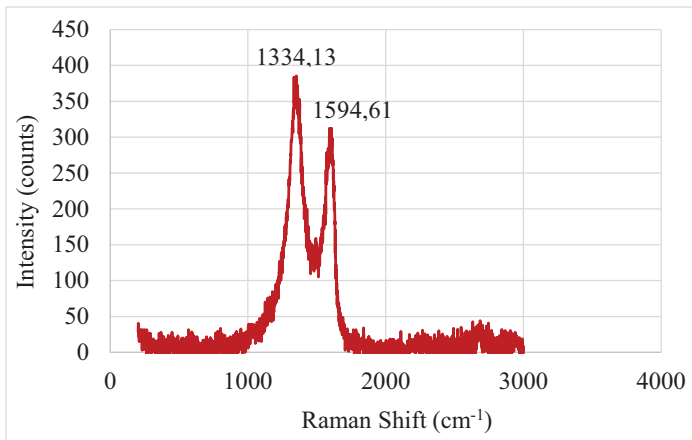


Fig. 4. Raman spectra of rGO/AgNPs

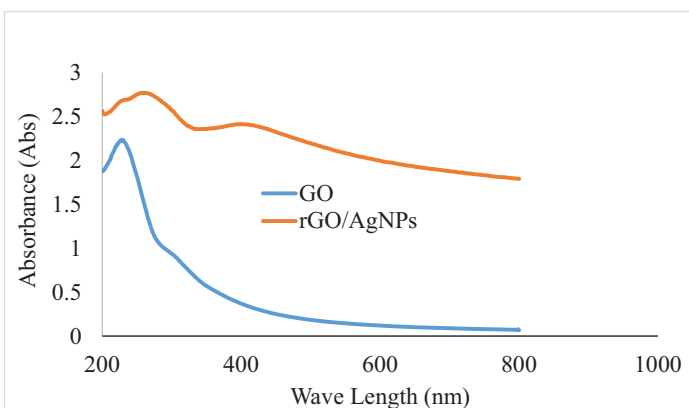


Fig. 5. UV-Vis spectra of GO and rGO/AgNPs

5. 2. Photocatalytic Activity Test

Performance of catalyst rGO/AgNP through the degradation process of Pb compounds in air by irradiating UV lamps as shown in the Fig. 6, 7.

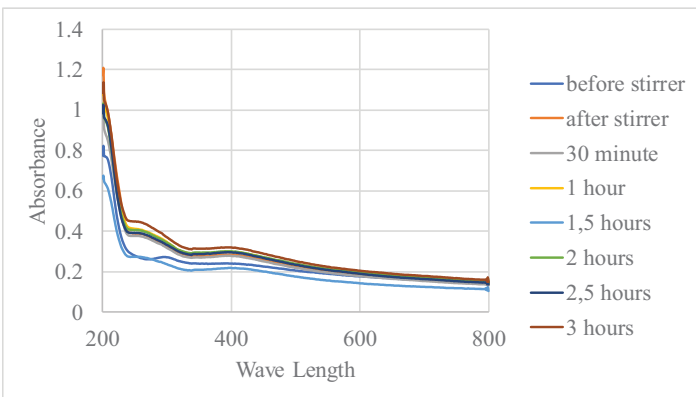
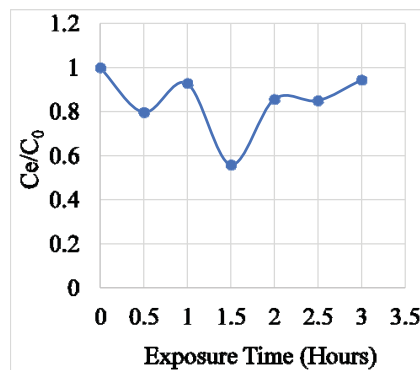


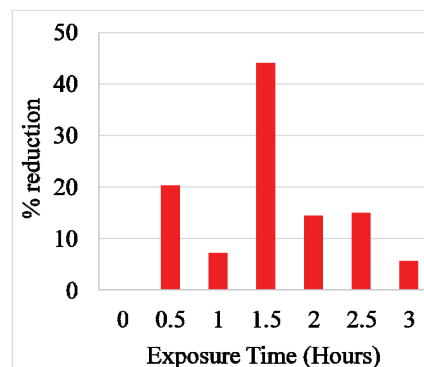
Fig. 6. Absorbance curve of photocatalytic activity test of rGO-AgNPs nanocomposite with NaBH₄ reducing agent

Fig. 6 shows photocatalytic performance test of rGO-AgNPs nanocomposite for the degradation of Pb Ion with the duration time of 3 hours.

Fig. 7 shows the amount of reduced Pb metal calculated by comparing its absorbance before and after being exposed to UV light in a dark room.



a



b

Fig. 7. The percentage of photocatalytic degradation versus times a – Ce/C₀ vs exposure time; b – %reduction vs exposure time

6. Discussion of synthesis of nanocomposites reduced graphene oxide-silver nanoparticles

Characterization of GO with XRD was carried out at 2θ=10°–100°. The result of XRD show in Fig. 1. The diffraction peak is found at 10,731° and a smaller peak at 26.448°. Based on the study, the diffraction peak for GO is 10.7° while the diffraction peak for graphite is 26.6° [32]. It can be concluded that in the sample, there is completely oxidized after treatment of the oxidation and exfoliation of graphite resulted the formation of oxygen-containing functional groups of graphene oxide [33, 34]

The XRD results of rGO/AgNPS is shown in Fig. 1. The diffraction peak is found at 38.1434°; 44.323°; 64.453°; and 77.385° for AgNPs and 26° for rGO. Based on the study, the diffraction peaks for nanocomposites AgNPs and their Miller indices were 38.08° (111), 44.16° (200), 64.44° (220), and 77.44° (311) [35] and for rGO it is in the range of 26.3° [36]. The Miller index and the diffraction pattern are derived from Ag nanoparticles in the form of a cube with a face-centered crystal structure. The loss of the GO identity diffraction peak at 10.7° indicates that GO has been reduced completely.

SEM images of the rGO/AgNPs nanocomposite were taken to study the morphology of the rGO/AgNPs nanocom-

posite structure. rGO has a thin layer of lamellar arrangement with a wrinkled surface and AgNPs spots in white dots [37]. These characteristics are seen in the SEM image of Fig. 4 with AgNPs spots which are clearly observed as white circle particles distributed on the surface of rGO in Fig. 2, *b*.

The EDX analysis result is shown in Fig. 3, which reveals that the rGO/AgNPs nanocomposites have been successfully obtained. The EDX result presents the compositions of the carbon (C) and oxygen (O) elements from rGO with the content of 53.9 % and 20.5 %, respectively. The Ag nanoparticles from AgNPs distributed on rGO was observed with the content of 25.5 %. Furthermore, no other elements are detected from EDX analysis showing the high purity of the synthesis result of rGO/AgNPs.

The Raman spectra of rGO/AgNPs are shown in Fig. 4. The D band shows the sp^3 carbon of defective sites and the G band reveals the plane vibrations with E_{2g} phonon. The rGO/AgNPs nanocomposites exhibits D bands at 1334,13 with intensity of 630,60 cm^{-1} and G band at 1594,61 with intensity of 477,29 cm^{-1} respectively. The I_D/I_G ratio for GO in our previous work is ~ 0.99 [25]. The I_D/I_G ratio rGO/AgNPs-rGO/AgNPs is ~1,32. The I_D/I_G of rGO/AgNPs nanocomposites increases due to the distribution of AgNPs on rGO surface [30].

The optical properties analysis of GO and rGO/AgNPs using UV-Vis was carried out by dissolving the nanocomposite in distilled water and measuring its absorbance at a wavelength of 200–800 nm and the result is depicted in Fig. 5. It is known that the synthesized GO has an absorbance peak at 227 nm and a small hump at ~300 nm. This indicates the presence of C=C and C=O structures in the synthesized GO. The second absorbance peak was found looking for a peak on the second derivative curve. The second absorbance peak is visible at a wavelength of 304 nm when the curve is lowered to order 2. Thus, it can be concluded that GO has been successfully synthesized.

In order to determine the peaks of the absorbance curve of the nanocomposite, the optical properties were also observed. Based on the study, rGO/AgNPs nanocomposite has an absorbance peak at a wavelength of 261 nm (red shift excitation $\pi-\pi^*$ of the C=C bond) and a smaller absorbance peak at 410 nm (AgNPs absorbance) [38]. Based on the result depicted in Fig. 5, it is observed that the synthesized rGO/AgNPs nanocomposite has absorbance peaks at 262 nm and 399 nm. This indicates the presence of C=C and Ag structures in the synthesized nanocomposite. The absence of a peak at 300 nm due to $n-\pi^*$ excitation of the C=O group indicates that GO has been reduced. Thus, it can be concluded that the rGO/AgNPs nanocomposite has been successfully synthesized.

In order to investigate the degradation of Pb ions and to know the maximum degradation of Pb ions, the observation of absorbance with the duration process of 3 hours by observing the absorbance intensity for every 30 minutes was conducted. The photocatalytic degradation performance is shown in the Fig. 6. The rGO-AgNPs peaks were seen at 260 nm and 400 nm. This experiment is supposed to reduce Pb^{2+} and produce Pb^0 species. This is in accordance with the study, which states that the peak at 200 nm comes from the interaction between carbon and Pb^{2+} [39].

Based on the calculation of the reduction rate (Fig. 7) it is known that the peak of reduction occurs at 1.5 hours of irradiation as the maximum degradation of Pb ions. As much as 44 % of the total initial concentration of Pb^{2+} in the con-

centration of 10 ppm was reduced to Pb^0 . This is indicated by the decreasing in the absorbance peak. In addition, the ratio of absorbance C_e/C_0 at 1.5 hours is the lowest compared to other irradiation times. However, the percentage of degradation Pb decreased on the duration of irradiation after 1.5 hours. This is because the reaction occurs in an equilibrium system. The electron holes in AgNPs react with the formed Pb^0 to convert it to Pb^{2+} again.

7. Conclusions

1. The result of SEM-EDX analysis showed that rGO has a thin layer of lamellar arrangement with a wrinkled surface and AgNPs spots in white dots are clearly observed as white circle particles distributed on the surface of rGO, with the elements of the carbon (C) and oxygen (O) from rGO is 53.9 % and 20.5 %, respectively. The Ag nanoparticles from AgNPs with the content of 25.5 % is observed with no other elements are detected from EDX analysis showing the high purity of the synthesis result of rGO/AgNPs. The XRD analysis for the synthesis GO and rGO/AgNPs with the diffraction peaks for nanocomposites rGO/AgNPs and their Miller indices were 38.08° (111), 44.16° (200), 64.44° (220), and 77.44° (311) indicating GO has been reduced and Ag nanoparticles in the form of a cube with a face-centered crystal structure.

2. The result of Raman spectra of rGO/AgNPs exhibits an I_D/I_G rGO/AgNPs ratio of ~1.32, indicating an increase in I_D/I_G due to the distribution of AgNPs on the rGO surface. So that the photocatalytic degradation performance described at 1.5 hours of irradiation resulted in the maximum ion degradation of Pb with a degradation efficiency of 44 %. The result of this study can be use the alternative nanophotocatalytic technology in waste treatment.

Conflict of interest

The authors declare that they have no conflict of interest in relation to this research, whether financial, personal, authorship or otherwise, that could affect the research and its results presented in this paper

Financing

The authors gratefully acknowledgements for the financial support provided by the Doctoral International Indexed Publication Grant (PUTI) 2020 from the University of Indonesia with contract number NKB-683/UN2.RST/HKP.05.00/2020.

Data availability

Manuscript has no associated data.

Acknowledgements

The research was carried out using laboratories at the Metallurgical Research Center, National Innovation Research Agency (BRIN) and material characterization from the analytical instrumentation facility ELSA (E-Layanan Sains).

References

1. Masindi, V., Muedi, K. L. (2018). Environmental Contamination by Heavy Metals. *Heavy Metals*. doi: <https://doi.org/10.5772/intechopen.76082>
2. Jaishankar, M., Tseten, T., Anbalagan, N., Mathew, B. B., Beeregowda, K. N. (2014). Toxicity, mechanism and health effects of some heavy metals. *Interdisciplinary Toxicology*, 7 (2), 60–72. doi: <https://doi.org/10.2478/intox-2014-0009>
3. Litter, M. I. (2015). Mechanisms of removal of heavy metals and arsenic from water by TiO₂-heterogeneous photocatalysis. *Pure and Applied Chemistry*, 87 (6), 557–567. doi: <https://doi.org/10.1515/pac-2014-0710>
4. Gusain, R., Kumar, N., Ray, S. S. (2020). Factors Influencing the Photocatalytic Activity of Photocatalysts in Wastewater Treatment. *Photocatalysts in Advanced Oxidation Processes for Wastewater Treatment*, 229–270. doi: <https://doi.org/10.1002/9781119631422.ch8>
5. Fröschl, T., Hörmann, U., Kubiak, P., Kučerová, G., Pfanzelt, M., Weiss, C. K. et al. (2012). High surface area crystalline titanium dioxide: potential and limits in electrochemical energy storage and catalysis. *Chemical Society Reviews*, 41 (15), 5313. doi: <https://doi.org/10.1039/c2cs35013k>
6. Setvín, M., Aschauer, U., Scheiber, P., Li, Y.-F., Hou, W., Schmid, M. et al. (2013). Reaction of O₂ with subsurface oxygen vacancies on TiO₂ anatase (101). *Science*, 341 (6149), 988–991. doi: <https://doi.org/10.1126/science.1239879>
7. Wang, L., Wei, H., Fan, Y., Liu, X., Zhan, J. (2009). Synthesis, Optical Properties, and Photocatalytic Activity of One-Dimensional CdS@ZnS Core-Shell Nanocomposites. *Nanoscale Research Letters*, 4 (6). doi: <https://doi.org/10.1007/s11671-009-9280-3>
8. Chen, P., Wang, F., Chen, Z.-F., Zhang, Q., Su, Y., Shen, L. et al. (2017). Study on the photocatalytic mechanism and detoxicity of gemfibrozil by a sunlight-driven TiO₂/carbon dots photocatalyst: The significant roles of reactive oxygen species. *Applied Catalysis B: Environmental*, 204, 250–259. doi: <https://doi.org/10.1016/j.apcatb.2016.11.040>
9. Lv, N., Li, Y., Huang, Z., Li, T., Ye, S., Dionysiou, D. D., Song, X. (2019). Synthesis of GO/TiO₂/Bi₂WO₆ nanocomposites with enhanced visible light photocatalytic degradation of ethylene. *Applied Catalysis B: Environmental*, 246, 303–311. doi: <https://doi.org/10.1016/j.apcatb.2019.01.068>
10. Fan, W., Zhou, Z., Wang, W., Huo, M., Zhang, L., Zhu, S. et al. (2019). Environmentally friendly approach for advanced treatment of municipal secondary effluent by integration of micro-nano bubbles and photocatalysis. *Journal of Cleaner Production*, 237, 117828. doi: <https://doi.org/10.1016/j.jclepro.2019.117828>
11. Kumar, A., Khan, M., Fang, L., Lo, I. M. C. (2019). Visible-light-driven N-TiO₂@SiO₂@Fe₃O₄ magnetic nanophotocatalysts: Synthesis, characterization, and photocatalytic degradation of PPCPs. *Journal of Hazardous Materials*, 370, 108–116. doi: <https://doi.org/10.1016/j.jhazmat.2017.07.048>
12. Kar, P., Zeng, S., Zhang, Y., Vahidzadeh, E., Manuel, A., Kisslinger, R. et al. (2019). High rate CO₂ photoreduction using flame annealed TiO₂ nanotubes. *Applied Catalysis B: Environmental*, 243, 522–536. doi: <https://doi.org/10.1016/j.apcatb.2018.08.002>
13. Méndez-Medrano, M. G., Kowalska, E., Lehoux, A., Herissan, A., Ohtani, B., Bahena, D. et al. (2016). Surface Modification of TiO₂ with Ag Nanoparticles and CuO Nanoclusters for Application in Photocatalysis. *The Journal of Physical Chemistry C*, 120 (9), 5143–5154. doi: <https://doi.org/10.1021/acs.jpcc.5b10703>
14. Kamat, P. V. (2011). Graphene-Based Nanoassemblies for Energy Conversion. *The Journal of Physical Chemistry Letters*, 2 (3), 242–251. doi: <https://doi.org/10.1021/jz101639v>
15. Yuan, L., Zhang, C., Zhang, X., Lou, M., Ye, F., Jacobson, C. R. et al. (2019). Photocatalytic Hydrogenation of Graphene Using Pd Nanocones. *Nano Letters*, 19 (7), 4413–4419. doi: <https://doi.org/10.1021/acs.nanolett.9b01121>
16. Guo, H., Jiang, N., Wang, H., Shang, K., Lu, N., Li, J., Wu, Y. (2019). Enhanced catalytic performance of graphene-TiO₂ nanocomposites for synergetic degradation of fluoroquinolone antibiotic in pulsed discharge plasma system. *Applied Catalysis B: Environmental*, 248, 552–566. doi: <https://doi.org/10.1016/j.apcatb.2019.01.052>
17. Russo, P., Hu, A., Compagnini, G. (2013). Synthesis, Properties and Potential Applications of Porous Graphene: A Review. *Nano-Micro Letters*, 5 (4), 260–273. doi: <https://doi.org/10.1007/bf03353757>
18. Pastrana-Martínez, L. M., Morales-Torres, S., Figueiredo, J. L., Faria, J. L., Silva, A. M. T. (2018). Graphene photocatalysts. Multifunctional Photocatalytic Materials for Energy, 79–101. doi: <https://doi.org/10.1016/b978-0-08-101977-1.00006-5>
19. Lee, C., Wei, X., Kysar, J. W., Hone, J. (2008). Measurement of the Elastic Properties and Intrinsic Strength of Monolayer Graphene. *Science*, 321 (5887), 385–388. doi: <https://doi.org/10.1126/science.1157996>
20. Mayorov, A. S., Gorbachev, R. V., Morozov, S. V., Britnell, L., Jalil, R., Ponomarenko, L. A. et al. (2011). Micrometer-Scale Ballistic Transport in Encapsulated Graphene at Room Temperature. *Nano Letters*, 11 (6), 2396–2399. doi: <https://doi.org/10.1021/nl200758b>
21. Park, S., Ruoff, R. S. (2009). Chemical methods for the production of graphenes. *Nature Nanotechnology*, 4 (4), 217–224. doi: <https://doi.org/10.1038/nnano.2009.58>
22. Morales-Torres, S., Pastrana-Martínez, L. M., Figueiredo, J. L., Faria, J. L., Silva, A. M. T. (2012). Design of graphene-based TiO₂ photocatalysts – a review. *Environmental Science and Pollution Research*, 19 (9), 3676–3687. doi: <https://doi.org/10.1007/s11356-012-0939-4>
23. Kamat, P. V. (2009). Graphene-Based Nanoarchitectures. Anchoring Semiconductor and Metal Nanoparticles on a Two-Dimensional Carbon Support. *The Journal of Physical Chemistry Letters*, 1 (2), 520–527. doi: <https://doi.org/10.1021/jz900265j>

24. Handayani, M., Mulyaningsih, Y., Aulia Anggoro, M., Abbas, A., Setiawan, I., Triawan, F. et al. (2022). One-pot synthesis of reduced graphene oxide/chitosan/zinc oxide ternary nanocomposites for supercapacitor electrodes with enhanced electrochemical properties. *Materials Letters*, 314, 131846. doi: <https://doi.org/10.1016/j.matlet.2022.131846>
25. Handayani, M., Suwaji, B. I., Ihsantia Ning Asih, G., Kusumaningsih, T., Kusumastuti, Y., Rochmadi, Anshori, I. (2022). In-situ synthesis of reduced graphene oxide/silver nanoparticles (rGO/AgNPs) nanocomposites for high loading capacity of acetylsalicylic acid. *Nanocomposites*, 8 (1), 74–80. doi: <https://doi.org/10.1080/20550324.2022.2054210>
26. Wang, N., Zhang, F., Mei, Q., Wu, R., Wang, W. (2020). Photocatalytic TiO₂/rGO/CuO Composite for Wastewater Treatment of Cr(VI) Under Visible Light. *Water, Air, & Soil Pollution*, 231 (5). doi: <https://doi.org/10.1007/s11270-020-04609-8>
27. Chong, M. N., Jin, B., Chow, C. W. K., Saint, C. (2010). Recent developments in photocatalytic water treatment technology: A review. *Water Research*, 44 (10), 2997–3027. doi: <https://doi.org/10.1016/j.watres.2010.02.039>
28. Sarina, S., Waclawik, E. R., Zhu, H. (2013). Photocatalysis on supported gold and silver nanoparticles under ultraviolet and visible light irradiation. *Green Chemistry*, 15 (7), 1814. doi: <https://doi.org/10.1039/c3gc40450a>
29. Tarcan, R., Todor-Boer, O., Petrovai, I., Leordean, C., Astilean, S., Botiz, I. (2020). Reduced graphene oxide today. *Journal of Materials Chemistry C*, 8 (4), 1198–1224. doi: <https://doi.org/10.1039/c9tc04916a>
30. Latiff, N. M., Fu, X., Mohamed, D. K., Veksha, A., Handayani, M., Lisak, G. (2020). Carbon based copper(II) phthalocyanine catalysts for electrochemical CO₂ reduction: Effect of carbon support on electrocatalytic activity. *Carbon*, 168, 245–253. doi: <https://doi.org/10.1016/j.carbon.2020.06.066>
31. Ciptasari, N. I., Darsono, N., Handayani, M., Soedarsono, J. W. (2021). Synthesis of graphite oxide using hummers method: Oxidation time influence. *AIP Conference Proceedings*. doi: <https://doi.org/10.1063/5.0061586>
32. Aliyev, E., Filiz, V., Khan, M. M., Lee, Y. J., Abetz, C., Abetz, V. (2019). Structural Characterization of Graphene Oxide: Surface Functional Groups and Fractionated Oxidative Debris. *Nanomaterials*, 9 (8), 1180. doi: <https://doi.org/10.3390/nano9081180>
33. Handayani, M., Sulistiyono, E., Rokhmanto, F., Darsono, N., Fransisca, P. L., Erryani, A., Wardono, J. T. (2019). Fabrication of Graphene Oxide/Calcium Carbonate/Chitosan Nanocomposite Film with Enhanced Mechanical Properties. *IOP Conference Series: Materials Science and Engineering*, 578 (1), 012073. doi: <https://doi.org/10.1088/1757-899x/578/1/012073>
34. Handayani, M., Kepakistan, K. A. A., Anshori, I., Darsono, N., Nugraha T., Y. (2021). Graphene oxide based nanocomposite modified screen printed carbon electrode for qualitative cefixime detection. *AIP Conference Proceedings*. doi: <https://doi.org/10.1063/5.0060625>
35. Zhang, L., Tan, Q., Kou, H., Wu, D., Zhang, W., Xiong, J. (2019). Highly Sensitive NH₃ Wireless Sensor Based on Ag-RGO Composite Operated at Room-temperature. *Scientific Reports*, 9 (1). doi: <https://doi.org/10.1038/s41598-019-46213-9>
36. Krisnandi, Y. K., Abdullah, I., Prabawanta, I. B. G., Handayani, M. (2020). In-situ hydrothermal synthesis of nickel nanoparticle/reduced graphene oxides as catalyst on CO₂ methanation. *AIP Conference Proceedings*. doi: <https://doi.org/10.1063/5.0007992>
37. Liu, G., Huang, L., Wang, Y., Tang, J., Wang, Y., Cheng, M. et al. (2017). Preparation of a graphene/silver hybrid membrane as a new nanofiltration membrane. *RSC Adv.*, 7 (77), 49159–49165. doi: <https://doi.org/10.1039/c7ra07904d>
38. Gurunathan, S., Han, J. W., Park, J. H., Kim, E., Choi, Y., Kwon, D., Kim, J. (2015). Reduced graphene oxide–silver nanoparticle nanocomposite: a potential anticancer nanotherapy. *Int J Nanomedicine*, 10 (1), 6257–6276. doi: <https://doi.org/10.2147/ijn.s92449>
39. Ciotta, E., Proposito, P., Tagliatesta, P., Lorecchio, C., Stella, L., Kaciulis, S. et al. (2018). Discriminating between Different Heavy Metal Ions with Fullerene-Derived Nanoparticles. *Sensors*, 18 (5), 1496. doi: <https://doi.org/10.3390/s18051496>